Short unligated sticky ends enable the observation of circularised DNA by atomic force and electron microscopies

Bernard Révet* and Alain Fourcade

Laboratoire de Microscopie Cellulaire et Moléculaire, CNRS URA 147, Institut Gustave-Roussy, F-94805 Villejuif Cedex, France

ABSTRACT

A comparative study of the stabilisation of DNA sticky ends by divalent cations was carried out by atomic force microscopy (AFM), electron microscopy and agarose gel electrophoresis. At room temperature, molecules bearing such extremities are immediately oligomerised or circularised by addition of Mg^{2+} or Ca^{2+}. This phenomenon, more clearly detected by AFM, requires the presence of uranyl salt, which stabilises the structures induced by Mg^{2+} or Ca^{2+}. DNA fragments were obtained by restriction enzymes producing sticky ends of 2 or 4 nucleotides (nt) in length with different guanine plus cytosine (GC) contents. The stability of the pairing is high when ends of 4 nt display a 100% GC-content. In that case, 95% of DNA fragments are maintained circular by the divalent cations, although 2 nt GC-sticky ends are sufficient for a stable pairing. DNA fragments with one blunt end and the other sticky appear as dimers in the presence of Mg^{2+}. Dimerisation was analysed by varying the lengths and concentrations of DNA fragments, the base composition of the sticky ends, and also the temperature. Our observation provides a new powerful tool for construction of inverted dimers, and circularisation, ligation analysis or short bases sequence interaction studies.

INTRODUCTION

No doubt, the most common technique used to analyse DNA cut by restriction endonucleases is to perform an agarose gel electrophoresis (AGE) of the reaction products. Another way is a direct observation and analysis of the DNA population by electron microscopy (EM) or more recent atomic force microscopy (AFM). Observation under the microscope gives the opportunity to monitor the cutting reaction continuously. However, when the population exceeds five fragments, measurements or counting can become very tedious.

As we have already shown, analysis of local curvature (1) or positioning of proteins interacting with a DNA molecule (2) is facilitated when the DNA fragment has been oriented, after specific incorporation at one end of a biotinylated nucleotide, by a streptavidin–ferritin complex (3). Labelling with either 5 nm streptavidin–gold spheres (4) or a chimerical streptavidin–immunoglobulin G-binding domain of staphylococcal protein A (5) has been proposed for analysis of biotinylated DNA molecules by AFM. Streptavidin alone, with no additional marker, is clearly visible in AFM and can be used for end-labelling (6). In order to avoid this requirement and its possible drawbacks, we prepared the molecules to be analysed using the following procedure. The DNA fragment was built in such a way that it possesses one blunt end and one sticky end; such fragments are then ligated with *Escherichia coli* ligase, which is active only on sticky-ended DNA fragments. The reaction product is a palindromic molecule twice the size of the original fragment. Consequently, any characteristic, such as a protein-specific binding site or a particular pattern (for instance a higher local curvature) will be observed twice on this molecule, at symmetrical positions.

For this procedure we originally used a 560 base pair (bp) DNA fragment which was rendered blunt at one end by *Pvu*II and sticky at the other by *Pst*I. Before performing the ligase reaction, we checked this DNA fragment by EM and by AFM. Under EM this fragment appeared as a 560 bp fragment with a length of 0.187 µm. But, under AFM, this DNA is often observed as a fragment measuring twice that length. This unexpected result is studied in detail here as a function of sticky end composition and length.

Ligation of DNA ends has been thoroughly studied in procedures where the process is catalysed by ligases, as discovered first by Gellert (7), or by topoisomerases (for a review see 8). In the case of bringing together DNA ends, many physical studies have been carried out in which sticky ends are involved, and mathematical models of this phenomenon have been proposed (9–12). However, until now the process has been analysed mainly with the use of DNA ligases.

In many biochemical processes, restricted DNA fragments are studied in the presence of a divalent cation, mainly Mg^{2+}. It has been also reported that Mg^{2+} stabilises nucleic acid structures such as three-way DNA junctions (13), DNA nicks (14), Z-DNA (15), RNA conformations (16,17) or ribozymes (18,19). Mg^{2+} ions also contribute to the winding of the DNA helix, as observed in supercoiled DNA molecules (20,21), and enhances DNA curvature (22,23).

---

*To whom correspondence should be addressed. Tel: +33 1 42 11 48 79; Fax: +33 1 42 11 52 76; Email: bmrevet@igr.fr

We have examined the behaviour of terminal ends of DNA restriction fragments and have analysed the effect of divalent cations on a population of such fragments. A comparative study has been made using AFM, EM and AGE. Numerous studies have been made on the stability of base pairs, mostly with short DNA (24) or RNA fragments (25). In this last study on short RNA duplex formation, a melting temperature of 22.6°C has been calculated for the sequence CCGG at 0.1 mM nucleotide in 1 M NaCl but hybridisation of the same sequence present at the extremities of short oligonucleotides has been observed in polyacrylamide gel at room temperature (26).

MATERIALS AND METHODS

DNA and restriction enzymes

All DNA fragments were prepared according to the following procedure. Samples of (5–10 µg) plasmid pSP65 or pUC19 DNA (a gift of J.M.Saucier) were cut with the restriction enzyme of interest (New England Biolabs, Beverly, MA, USA) until completion as judged by EM observation. Proteinase K (Boehringer Mannheim, Meylan, France) at a final concentration of 20 µg/ml was added to the tubes, and incubation at 37°C was continued for 1 h. The samples were then loaded on a MonoQ column and fractionated according to size on a Smart system (Pharmacia Biotech, Uppsala, Sweden) with a NaCl gradient (0.7–0.85 M). The fractions of interest were pooled and precipitated with ethanol. The precipitated fragments were resuspended in Te buffer (10 mM Tris, pH 8, 0.1 mM EDTA).

Electrophoresis

Electrophoresis of the DNA fragments were performed on mini 1% agarose (SeaKem LE, FMC Bioproducts, Rockland, ME, USA) slab gels (GIBCO BRL Life Technologies, Cergy Pontoise, France) in TAE buffer (40 mM Tris base, 0.1 mM NaEDTA, 20 mM sodium acetate, 29.6 mM glacial acetic acid, pH 7.8) with or without MgCl$_2$ (10 mM). pSP65 plasmid DNA with all three natural forms (I supercoiled, II circular relaxed and III linear) was added in one well as markers. Electrophoresis was run in the cold for 3–4 h at 4 V/cm. The gels were stained with SYBR Green I (Molecular Probes Europe BV, Leiden, The Netherlands) and photographed using a yellow filter on Polaroid 667 films.

Electron microscopy

DNA samples (7 µl; ~1 µg/ml) in Te buffer with or without 10 mM MgCl$_2$ were spread onto pentylamine-activated carbon-coated grids, washed and stained with 2% (w/v) uranyl acetate solution in water and dried on filter paper (27). When necessary uranyl acetate was added to the sample at a final concentration of 24 µM (see text). Grids were observed by use of annular dark-field illumination mode with a Zeiss CEM-902 microscope (28). Images were recorded on Kodak electron image film (Eastman Kodak, Rochester, NY, USA) at a magnification of 50 000 or 85 000×.

Atomic force microscopy

Samples of DNA were generally prepared as described by Delain *et al.* (29) with some modifications. DNA (~1 µg/ml) was diluted in 10 mM Tris, pH 7.4, 10 mM MgCl$_2$. Five microliters were deposited onto a freshly cleaved mica (five different micas

including ruby type were used with similar results). After 1 min the sample was rinsed with 2–3 drops of 0.2% (w/v) aqueous uranyl acetate, blotted with paper and dried. For experiments in which the possible role of uranyl salt was examined, thorium nitrate (0.0001%, w/v), an alternative to uranyl acetate for DNA spreading and staining (30), was used in place of uranyl acetate or in association with a very low concentration of it, as indicated. In some experiments we used the technique described by Rivetti *et al.* (31), in which DNA was diluted in 4 mM HEPES pH 7.5, 10 mM NaCl, 2 mM MgCl$_2$, deposited onto ruby mica for 2 min and rinsed with 10 ml of water with a syringe through a needle, blotted and dried. Following this last technique, we changed the rinsing procedure by replacing water with 10 ml of 10 mM MgCl$_2$ or by an uranyl acetate rinse as used in our own protocol. For the temperature experiments, mica, uranyl acetate, the DNA solution and micropipettes were prewarmed to 50, 60 or 70°C in an incubator for 20 min before sample preparation. Observations were performed with a NanoScope IIIa (Digital Instruments, Santa Barbara, CA, USA) in the Tapping® mode in air, using standard TESP silicon tips. Fields of 1–4 µm were scanned at a maximum frequency of 1.5 Hz. Images (512 × 512) were flattened and exported as TIFF files to Adobe PhotoShop 4.0 for document preparation.

Population analysis and data

NanoScope images were imported on a MacIntosh Performa 6400/180 using the public domain NIH Image 1.61 (written by Wayne Rasband at the US National Institute of Health). Images of DNA molecules were treated using dedicated macros written by us. First they were individually cleaned (with verification against the NanoScope original image), then skeletonised, and finally length was measured on 100–300 molecules. Globally, our measurement method underestimates length by ~1% for small fragments (<500 nm) to ~6% (length >1 µm) as compared to the theoretical values calculated with 0.34 nm/bp. After counting, population analysis results were expressed in three different ways. Firstly, as a percentage of circularised forms, including monomers, dimers or larger oligomers. Secondly, as a percentage of oligomers of all sizes, either linear or circular. Lastly, as a percentage of paired sticky ends, which represents the whole reassociation of complementary sticky ends of the fragments, whatever the resulting form.

RESULTS

Table 1 summarises the results obtained in AFM for the DNA fragments, as a function of the sticky ends employed. In this table the samples preparation for AFM observation was always done according to our method including the uranyl acetate rinse.

Dimerisation of DNA fragments having one sticky end and one blunt end

Influence of the GC content. First, we analysed the influence of the GC content of the sticky end on the dimerisation of DNA fragments having one sticky end and one blunt end. The following DNA fragments: *Pvu*II (blunt)–*Eco*RI (0% GC), *Pvu*II (blunt)–*Sph*I (50% GC) and *Pvu*II (blunt)–*Ngo*MI (100% GC) were used for this analysis. Dimerisation was observed in all cases (Fig. 1D and E) shows examples of dimerisation of the *Pvu*II–*Ngo*MI small fragment (511 bp) and of the *Pvu*II–*Sph*I

Table 1. Plasmid DNAs and restriction enzymes used, fragment characteristics, number of molecules studied by AFM and results of sticky ends base pairing

Enzymes	Ends		GC % of sticky ends	Fragment size bp	Number of molecules	Cyclisation	Oligomerisation	Paired sticky ends
				pSP65 DNA plasmid				
*Pvu*II	blunt			226	232	No	67% (D)	80%
*Eco*RI	sticky	TTAA	0					
*Pvu*II	blunt			672	431	No	49% (D)	63%
*Sph*I	sticky	CATG	50	2333	794		30% (D)	47%
*Pvu*II	blunt			511	306	No	54% (D)	70%
*Ngo*MI	sticky	GGCC	100					
*Eco*RI	sticky	AATT		3005	212	47% (M,D)	9% (D,O)	50%
	sticky	TTAA	0					
*Aat*II	sticky	TGCA		3005	276	60% (M,D)	24% (D,O)	72%
	sticky	ACGT	50					
*Ngo*MI	sticky	CCGG		3005	232	95% (M,O)	11% (D,O)	95%
	sticky	GGCC	100					
*Apa*LI	sticky	TGCA		497	242	82% (M,O)	10% (D,O,MO)	83% (a)
	sticky	ACGT	50	1246,1262		87% (M,O)		87% (b)
*Nhe*I	sticky	CTAG		534	103	14% (D)	35% (D)	36%
*Aat*II	sticky	ACGT	50/50 (c)					
*Psp*1406I	sticky	CG		373	207	27% (M,O)	55% (D,O,MO)	68% (a)
	sticky	GC	100	2632		40% (M)		
				pUC19 DNA plasmid				
*Nde*I	sticky	TA		2686	96	No	No	0%
	sticky	AT	0					

Abbreviations: M, monomer; D, dimer; O, oligomer; MO, mixed oligomer. The restricted overhanging sequences which can pair (stick) are indicated and underlined. (a) Includes only circular monomers, and homo-oligomers of the small fragment which size is less than that of the large fragment monomer cannot be determined for the few large oligomeric fragments because of the great variety of sizes due to mixed oligomers. (b) Restricted to circular monomers, and dimers of the large fragments (1246 plus 1262 bp, which are not distinguishable) for the same reason as for (a). (c) The two generated sticky ends are not self-complementary

large fragment (2333 bp), respectively. At room temperature, for the small DNA fragments (226–672 bp) slight differences in the percentage of dimers formed (Table 1) were observed; but they may be attributed mainly to size, and to concentration variations. Thus, as expected the large *Pvu*II–*Sph*I fragment (Fig. 1E) shows a lower percentage of dimers than the small *Pvu*II–*Ngo*MI fragment.

Effect of temperature. The stability of the sticky end base pairing as a function of temperature was determined with the following AFM experiments. Small DNA fragments, such as the one used above, were incubated and deposited at ~25 (room temperature), 50, 60 or 70°C. For the small *Pvu*II (blunt)–*Eco*RI (sticky, 0% GC) fragment the percentage of dimers decreases from 67% at 25°C to 48% at 50°C and to 8% at 60°C. Similar results were obtained with the small *Pvu*II (blunt)–*Sph*I (sticky, 50% GC) fragment for which the percentages of dimers were 49, 53 and 6%, respectively. In contrast, for the small *Pvu*II (blunt)–*Ngo*MI (sticky, 100% GC) fragment the percentage of dimers decreases only from 55% at 25°C to 35% at 60 and 70°C must be reached for the dimer percentage to decrease to 10%.

Circularisation of DNA fragments having two sticky ends

When the two ends of the fragments are sticky and complementary, circularisation was observed in almost all cases. It was also seen when the two ends of the fragment are sticky and not complementary; but in this case oligomer formation takes place in order to allow cyclisation of paired oligomers giving rise to large circles (Fig. 1A–C and F; Table 1).

pSP65 DNA was cut with single cut restriction enzymes giving 4 nt sticky ends of different GC percentage in fragments of the same size (3005 bp). An analysis of the molecular population cut at the unique *Ngo*MI site (100% GC) shows that 95% of the molecules are circularised and 87% are monomer circles (Fig. 1C). When the DNA was cut with the restriction enzyme *Aat*II (50% GC) 60% of the molecules are circularised, either as monomers or dimers. Finally, for the population which corresponds to the unique site *Eco*RI (0% GC) the percentage of circles drops to 47% (Fig. 1A).

pSP65 DNA was then cut with the restriction enzyme *Apa*LI (50% GC), which forms three fragments (497, 1246 and 1262 bp), but only two populations distinguishable because the two large fragments differ only by 1% in length. In this case, a large percentage of circles is still observed: 82% for the small fragment and 87% for the large ones (Fig. 1B). We also observed a small fraction of circles (5%) corresponding to an oligomerised combination of the fragments. The pSP65 plasmid DNA was also simultaneously cut with the two restrictions enzymes *Nhe*I and *Aat*II which give two fragments (534 and 2471 bp) with non-self-complementary 4 nt sticky ends. The population distribution of the small fragments shows that 65% are monomers and 35% dimers, among which 39% are circularised. We then cut the plasmid DNA with the enzyme *Psp*1406I which gives two fragments (373 and 2632 bp) with only 2 nt GC-sticky ends; we still observed a significant percentage of circularised fragment: 40% of large fragment monomers and 27% of small fragment monomers, dimers or trimers (Fig. 1F). Finally, when plasmid pUC19 DNA was cut with *Nde*I which produces one single fragment with 2 nt AT-sticky ends no circles were found.

Oligomerisation of DNA fragments having two sticky ends

DNA fragments having two sticky ends can also attach to another one. When the pSP65 plasmid was cut with *Ngo*MI (100% GC content) 11% of the molecules were found to form linear or circular oligomers (Fig. 1C). If the plasmid is cut with *Aat*II (50% GC content), the percentage of oligomers equals 24%; and for the plasmid cut with *Eco*RI (0% GC content), the percentage of oligomers equals 9% (Fig. 1A). When the plasmid was cut with the enzyme *Apa*LI (50% GC content) which gives two distinguishable populations of fragment the total percentage of oligomers equals 10% (Fig. 1B). For 2 nt 100% GC-sticky ends (pSP65 plasmid DNA cut with *Psp*1406I), the percentage of oligomers was high (55%) and 68% of the sticky ends carried by the small fragment were paired in circles or oligomers (Fig. 1F). In contrast, 100% AT content 2 nt sticky-ended fragments (pUC19 plasmid DNA cut with *Nde*I), presented the only case in which annealing was never observed.

Role of electric charges, and magnesium and uranyl ions on sticky ends pairing

Since circularisation or oligomerisation of sticky ends were not noticed previously by conventional EM or AFM, we further consider what could be the reason of this discrepancy. We looked particularly for the role of electric charges, and of magnesium and uranyl ions in sticky ends pairing. In EM, the carbon film is charged in the presence of pentylamine (27) to attach and spread the DNA; and after adsorption the DNA is washed with an aqueous uranyl acetate solution. In AFM, we also washed the sample with uranyl acetate; this is not commonly used, except in one published work on ΦX-174 single-stranded DNA (32). We
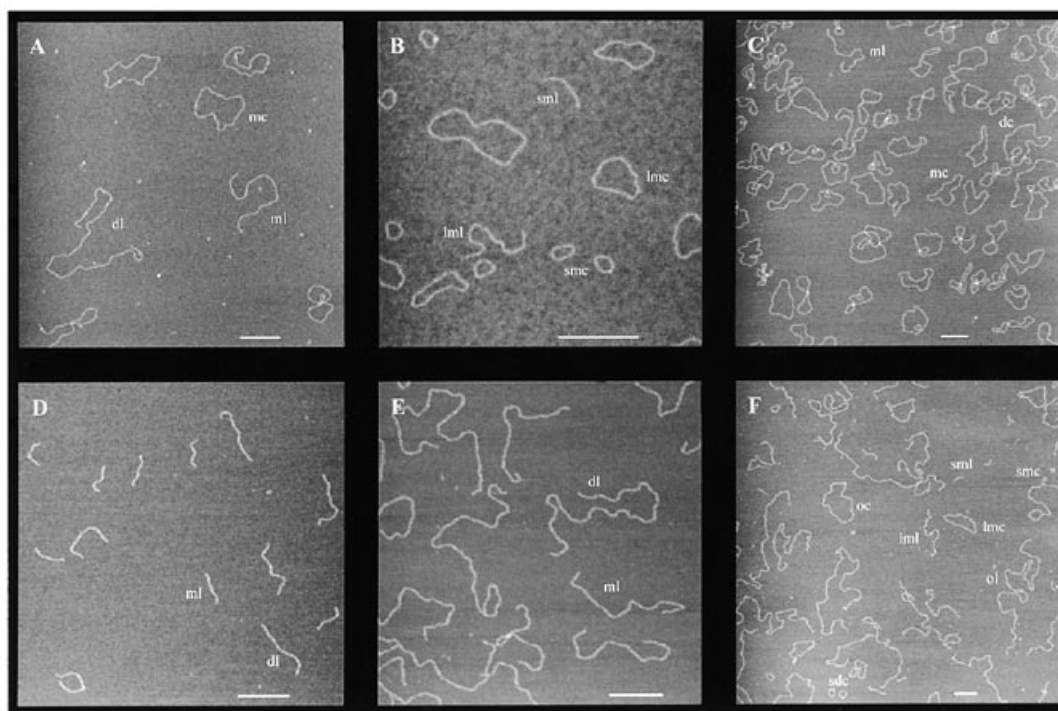
Figure 1. Atomic force microscopy images of pSP65 DNA fragments deposited onto mica, appearing as linear or circular monomers, dimers or higher oligomers. (**A**) *Eco*RI 3005 bp fragment. (**B**) *Apa*LI 497 and 1246–1262 bp fragments (not distinguishable after measurements). (**C**) *Ngo*MI 3005 bp fragment. (**D**) *Pvu*II–*Ngo*MI small fragment (511 bp). (**E**) *Pvu*II–*Sph*I large fragment (2333 bp). (**F**) *Psp*1406I mixture of small and large fragments (373 and 2632 bp). Abbreviations used to outline particular features: (m) monomer, (sm) small monomer, (lm) large monomer, (d) dimer, (o) oligomer; as last letter: (l) linear, (c) circular; Bar, 0.25 μm.

performed EM and AFM experiments to study the effect of cations, and tried also to demonstrate reassociated DNA molecules by AGE.

Electron microscopy. To analyse separately the effect that Mg^{2+} or UO_2^{2+} ions could have on the sticky ends of the DNA fragments, we added a small quantity of uranyl acetate (final concentration 24 μM) to the DNA sample before deposition onto the previously charged grid, and the sample was washed with the 2% aqueous uranyl acetate, as usual. Under EM, in the case of the plasmid DNA cut by *Ngo*MI, 90% of the molecules were circles if Mg^{2+} or Ca^{2+} were present in the deposit (Fig. 2B). For *Aat*II (Fig. 2C and D) or *Eco*RI fragments, the percentages of circles were 30 and 10%, respectively, lower than that observed under AFM (Table 1). Here, besides the circles, many open molecules have their ends in a very close proximity, indicating that rupture of the paired sticky ends happened at the time of adsorption onto the treated carbon film (arrows on Fig. 2C and D). Under EM with or without the small quantity of uranyl acetate, added to the DNA sample before deposition, no circles were observed if the divalent cations were omitted (Fig. 2A).

Atomic force microscopy. In an AFM experiment, the uranyl acetate concentration used for rinsing was lowered until only partial spreading of *Ngo*MI cut DNA was observed (0.0002%, 4.7 μM). If we then add thorium nitrate (final concentration 1.7 μM), which is another DNA staining and spreading agent used for EM (30), to this low concentration of uranyl acetate, then circles are clearly observed, but in lesser amount probably related to the decrease of the UO_2^{2+} concentration. Thorium alone, at the same concentration, did not result in the detection of any circular

molecules. AFM experiments were also done at lower Mg^{2+} concentrations; at 5 and 2 mM $MgCl_2$ there was no difference in the observed populations. At lower concentrations, DNA does not attach homogeneously to the mica.

Agarose gel electrophoresis. We then used agarose gel electrophoresis of DNA samples diluted in TAE buffer containing 10 mM $MgCl_2$ (Fig. 3). The agarose gel and the TAE running buffer also contained 10 mM $MgCl_2$. The chosen DNA have sticky ends of varying GC content. After migration of the DNA cut by *Ngo*MI (100% GC sticky end), in the cold at low voltage, a smear was present between the positions of the linear (form III) and the nicked (form II) plasmid DNA (Fig. 3, lane A). The circularised molecule dissociates to the linear form during the migration. A light smear was also observed in the *Eco*RI (0% GC content) cut plasmid (Fig. 3, lane B). The *Aat*II (50% GC content) cut plasmid also showed a band at the position of the linear plasmid DNA (Fig. 3, lane E), but no smear was observed on the gel presented, due to the lower amount of DNA in the band (Fig. 3, lane C). Plasmid DNA which was cut with *Psp*1406I showed two bands corresponding to the fragments 373 and 2632 bp (Fig. 3, lane D). The slowly migrating band also presented a light smear behind it. When uranyl acetate (final concentration 0.0004%, 9.4 μM) was added to the gel, the samples and the running buffer, which all also contained 10 mM Mg^{2+}; similar results were obtained (data not shown), except that more material remained in the wells, indicating that some DNA precipitation occurred. In absence of Mg^{2+}, no smears were observed, and the *Ngo*MI, *Eco*RI and *Aat*II cut plasmid DNAs all migrated at the position of the natural linear form III (data not shown).
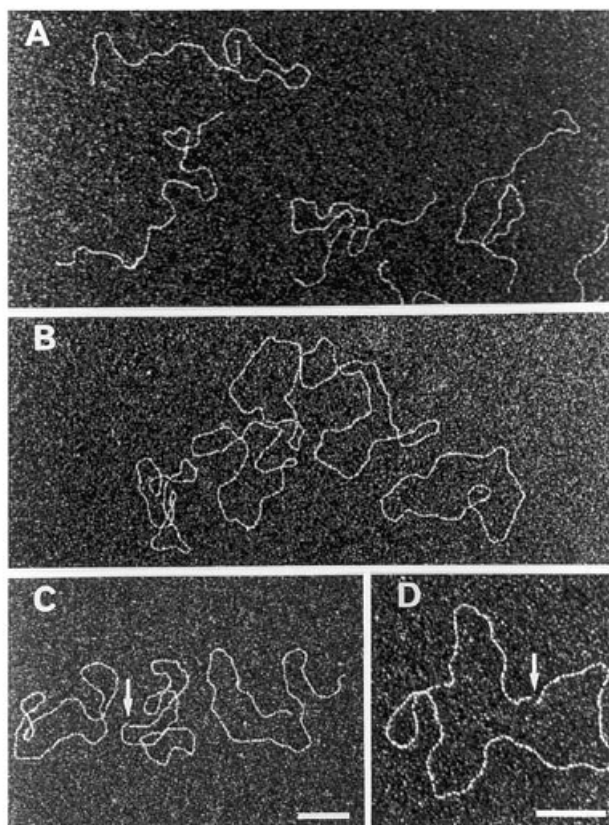
Figure 2. Electron microscopy dark-field images of pSP65 DNA fragment (3005 bp). (**A**) Fragment cut by *Ngo*MI in Te buffer as in usual EM preparation (without MgCl$_2$ or CaCl$_2$). (**B**) Same fragment as (A) but in Te buffer containing 23 µM uranyl acetate plus 10 mM CaCl$_2$. (**C** and **D**) Fragment cut by *Aat*II in the same buffer as (B) but with 10 mM MgCl$_2$ instead of CaCl$_2$ (the arrows mark the disruption of some DNA circles). (A–C) Magnification Bar, 0.1 µm.

Figure 3. Agarose gel electrophoresis of pSP65 DNA cut by different restriction enzymes and run in the presence of 10 mM MgCl$_2$. Lane A, *Ngo*MI fragment (3005 bp). Lane B, *Eco*RI fragment (3005 bp). Lane C, *Aat*II fragment (3005 bp). Lane D, *Psp*1406I fragments (373 and 2632 bp). Lane E, untreated DNA (3005 bp) showing a mixed population of superhelical, relaxed and linear molecules (forms I, II and III, respectively). The fragments size and the plasmid DNA forms are indicated on the left or on the right side, respectively.

DISCUSSION

From the above results, we conclude that the divalent cation Mg^{2+} (or Ca^{2+}) keeps together the sticky ends of the restricted fragments giving rise to their circularisation or their oligomerisation. Such a phenomenon was clearly observed under AFM when the material deposited onto the mica was washed with aqueous uranyl acetate. The occurrence of dimer formation through a four dG·dC base pair overhang has been observed in *Xma*I DNA fragments by polyacrylamide gels (26). But to our knowledge, circularisation or oligomerisation of DNA restriction fragments has not been visualized before by EM or AFM. Such sticky-ended DNA fragments have been used in the presence of Mg^{2+} ions in many AFM experiments (31–35). In our hands, using the conditions of Rivetti *et al.* (31), we also did not observe any interactions between DNA sticky ends, except when the final rinse of the sample was performed with uranyl acetate instead of water.

In agarose gel, when Mg^{2+} ions are present, the smears observed can be interpreted as an indication that the pre-existing structures in the presence of Mg^{2+}, are partly destabilised during the migration.
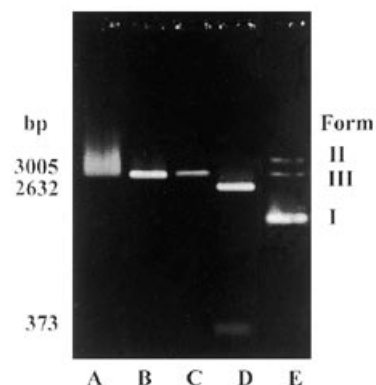
In EM, the carbon-coated grids are commonly charged in the presence of pentylamine (27), and the presence of positive charges on the grid could destabilise the sticky ends. During the deposition process there is adsorption to the grid at a given number of points along the DNA, followed by structural rearrangement of the molecule. The involved forces are probably stronger than the hydrogen bonding of the sticky ends. Moreover, after adsorption of the DNA sample onto the carbon film, the sample is commonly washed with an aqueous uranyl acetate solution. Consequently, one observes the precipitates of uranium atoms as clusters on the phosphate backbone (30). In AFM, under our own conditions, we also washed the sample with uranyl acetate. Thus, it appears that divalent ions such as magnesium and uranyl could play a role in sticky ends base pairs stabilisation. Under EM, using the glow-discharge method (27), uranyl acetate at a very low concentration must be added to the sample before deposit in order to reveal the presence of circularised or oligomerised molecules. Our hypothesis is that the large clusters of 10–20 uranium atoms (30) may reinforce the structures which have already been stabilised by the Mg^{2+} ion, possibly by binding to more distant negative phosphate sites of both strands. This property is not shared by the monovalent thorium nitrate salt.

The concentration of DNA fragments, or of sticky ends, is an important factor in the annealing of the molecules. For instance, at high concentrations, as in a DNA stock solution at ~100 µg/ml, reassociation between sticky ends of different molecules is favoured, giving rise to oligomers. DNA samples are usually dissolved and analysed in buffers containing EDTA. We observed that if a stock solution containing MgCl$_2$ is diluted in a buffer containing Mg^{2+}, larger sized oligomers (linear tetramers and over) are seen as opposed to a stock solution with no MgCl$_2$ and with 10 mM EDTA, even if the percentage of circularised monomers is about the same. From this observation, we can conclude that reassociation is a rapid process, since it occurred during the 5 min needed to dilute and prepare the AFM sample. Another important factor is the size of the fragments, as observed during the dimerisation of small fragments. The very short (226 bp) *Pvu*II–*Eco*RI (0% GC content) fragments dimerised more

efficiently than the longer (511 bp) *Pvu*II–*Ngo*MI (100% GC content) fragment. A third important parameter affecting the base pairing of sticky ends belonging to DNA fragment of given size, is their base composition and, notably their GC-content.

The data presented indicate that in the presence of the divalent Mg^{2+} or Ca^{2+} ions, annealing of the sticky ends is extremely efficient when they are 100% GC as with *Ngo*MI (4 nt sticky ends). Consequently, one might expect that association of independent molecules is not favoured in this case, and that circularisation of molecules is highly probable. Even with 2 nt GC-sticky ends (*Psp*1406I) reassociation is frequent, giving rise to oligomers and circles. In contrast, 2 nt AT-sticky ends, as shown with *Nde*I, are very unstable, which indicates that association rarely occurs with such molecules. The most favourable conditions for observing shuffling of DNA fragments to form combined species is thus 4 nt sticky ends with a 50% GC- or a 100% AT-content.

When fragments having identical 100% GC-sticky ends are put in the presence of ligase, ligating them into circles should be very efficient, since 95% of the fragments are already circularised, as shown here, before the addition of the ligase. In ligation experiments, joining of the sticky ends and base pairing prevail over the ligature step. Due to the high stability of sticky end pairing we detect, one should always take into account the key role of the divalent cation on the molecules in biochemical processes; for instance, in the joining of *Eco*RI DNA fragments by the protein Ku (35) or, in recombination experiments with RecA, in which the observation of chiasma is probably not only due to the high efficiency of polymerisation of RecA but also to the high tendency of oligomerisation of the DNA fragments with sticky ends used (17,36–38). As a consequence, differences in the recombination process may occur depending the nature of the ends of the DNA fragments.

The phenomenon described here provides a new tool for studying DNA. Firstly, the use of magnesium-stabilised inverted symmetrical dimers (in place of enzymatically ligated ones) permits the local curvature analysis of a selected DNA fragment without the need for end-labelling (A.Fourcade and B.Révet, in preparation). Such dimers also offer the possibility of discriminating between non-specific binding sites and specific ones by the symmetrical localisation of the ligand. Secondly, the pairing between sticky ends of the same DNA fragment should be very helpful in circularisation or ligation experiments, since it allows the independent study of the recognition steps, without any enzymatic ligation. Lastly, subtle base pair interaction could be analysed on very short sticky ends which sequence contains normal or modified bases.

The present work offers a new possibility of analysing base pair stability in short DNA sequences and could be extended to other methods by the use of synthetic oligomers with sticky ends permitting studies of hydrogen bonding, base pair stacking and charge neutralisation. It also allows the analysis of the first process which takes place in ligation experiments as the products concerned, circularised or oligomerised fragments, can be analysed before the enzymatic event. It finally shows the important role of Mg^{2+} in stabilisation of DNA terminal ends. We hope also that our observation will initiate a large number of questions and investigations about the behaviour of isolated sticky-ended DNA fragments.

REFERENCES

1. Muzard,G., Théveny,B. and Révet,B. (1990) *EMBO J.*, **9**, 1289–1298.
2. Révet,B., Brahms,S. and Brahms,G. (1995) *Proc. Natl. Acad. Sci. USA*, **92**, 7535–7539.
3. Théveny,B. and Révet,B. (1987) *Nucleic Acids Res.*, **15**, 947–958.
4. Shaiu,W.-L., Larson,D.D., Vesenka,J. and Henderson,E. (1993) *Nucleic Acids Res.*, **21**, 99–103.
5. Murray,M.N., Hansma,H.G., Benazilla,M., Sano,T., Ogletree,D.F., Kolbe,W., Smith,C.L., Cantor,C.R., Spengler,S., Hansma,P.K. and Salmeron,M. (1993) *Proc. Natl. Acad. Sci. USA*, **90**, 3811–3814.
6. Cherny,D.I., Fourcade,A., Svinarchuk,F., Nielsen,P.E., Malvy,C. and Delain,E. (1998) *Biophys. J.*, **74**, 1015–1023.
7. Gellert,M. (1967) *Proc. Natl. Acad. Sci. USA*, **57**, 148–155.
8. Wang,J.C. (1996) *Annu. Rev. Biochem.*, **65**, 635–692.
9. Wang,J.C. and Davidson,N. (1966) *J. Mol. Biol.*, **19**, 469–482.
10. Dugaiczyk,A., Boyer,H.W. and Goodman,H.M. (1975) *J. Mol. Biol.*, **96**, 171–184.
11. Shore,D. and Baldwin,R.L. (1983) *J. Mol. Biol.*, **170**, 957–981.
12. Taylor,W.H. and Hagerman,P.J. (1990) *J. Mol. Biol.*, **212**, 363–376.
13. Leontis,N.B., Kwok,W. and Newman,J.S. (1991) *Nucleic Acids Res.*, **19**, 759–766.
14. Le Cam,E., Fack,F., Ménissier-de Murcia,J., Cognet,J.A.H., Barbin,A., Sarantoglou,V., Révet,B., Delain,E. and de Murcia,G. (1994) *J. Mol. Biol.*, **235**, 1062–1071.
15. Révet,B., Delain,E., Dante,R. and Niveleau,A. (1983) *J. Biomol. Struct. Dynam.*, **1**, 857–871.
16. Laing,L.G., Gluick,T.C. and Draper,D.E. (1994) *J. Mol. Biol.*, **237**, 577–587.
17. Marquet,R., Baudin,F., Gabus,C., Darlix,J.-L., Mougel,M., Ehresmann,C. and Ehresmann,B. (1991) *Nucleic Acids Res.*, **19**, 2349–2352.
18. Tinoco,I.,Jr and Kieft,J.S. (1997) *Nature Struct. Biol.*, **4**, 553–558.
19. Cate,J.H., Hanna,R.L. and Douda,J.A. (1997) *Nature Struct. Biol.*, **4**, 553–558.
20. Bednar,J., Furrer,P., Stasiak,A., Dubochet,J., Egelman,E.H. and Bates,A.D. (1994) *J. Mol. Biol.*, **235**, 825–847.
21. Xu,Y.-C. and Bremer,H. (1997) *Nucleic Acids Res.*, **25**, 4067–4071.
22. Diekmann,S. (1987) *Nucleic Acids Res.*, **15**, 247–265.
23. Révet,B.M.J., Sena,E.P. and Zarling,D.A. (1993) *J. Mol. Biol.*, **232**, 779–791.
24. Breslauer,K.J., Frank,R., Blöcker,H. and Marky,L.A. (1986) *Proc. Natl. Acad. Sci. USA*, **83**, 3746–3750.
25. Freier,S.M., Kierzek,R., Jaeger,J.A., Sugimoto,N., Caruthers,M.H., Neilson,T. and Turner,D.H. (1986) *Proc. Natl. Acad. Sci. USA*, **83**, 9373–9377.
26. Klysik,J., Rippe,K. and Jovin,T.M. (1991) *Nucleic Acids Res.*, **19**, 7145–7154.
27. Dubochet,J., Ducommun,M., Zollinger,M. and Kellenberger,E. (1971) *J. Ultrastruct. Res.*, **35**, 147–167.
28. Delain,E., Fourcade,A., Révet,B. and Mory,C. (1992) *Microsc. Microanal. Microstruct.*, **3**, 175–186.
29. Delain,E., Fourcade,A., Poulin,J.-C., Barbin,A., Coulaud,D., Le Cam,E. and Paris,E. (1992). *Microsc. Microanal. Microstruct.*, **3**, 457–470.
30. Mory,C., Colliex,C., Révet,B. and Delain,E. (1981) *Ultramicroscopy*, **7**, 161–168.
31. Rivetti,C., Guthold,M. and Bustamante,C. (1996) *J. Mol. Biol.*, **264**, 919–932.
32. Hansma,H.G., Laney,D.E., Bezanilla,M., Sinsheimer,R.L. and Hansma,P.K. (1995) *Biophys. J.*, **68**, 1672–1677.
33. Wyman,C., Grotkopp,E., Bustamante,C. and Nelson,H.C.M. (1995) *EMBO J.*, **14**, 117–123.
34. Coury,J.E., McFail-Isom,L., Williams,L.D. and Bottomley,L.A. (1996) *Proc. Natl. Acad. Sci. USA*, **93**, 12283–12286.
35. Pang,D., Yoo,S., Dynan,W.S., Jung,M. and Dritschilo,A. (1997) *Cancer Res.*, **57**, 1412–1415.
36. Flory,J. and Radding,C.M. (1982) *Cell*, **28**, 747–756.
37. Rao,B.J., Dutreix,M. and Radding,C.M. (1991) *Proc. Natl. Acad. Sci.*, *USA*, **88**, 2984–2988.
38. Register,J.C. III and Griffith,J. (1986) *Proc. Natl. Acad. Sci.*, *USA*, **83**, 624–628.